FIG. 1

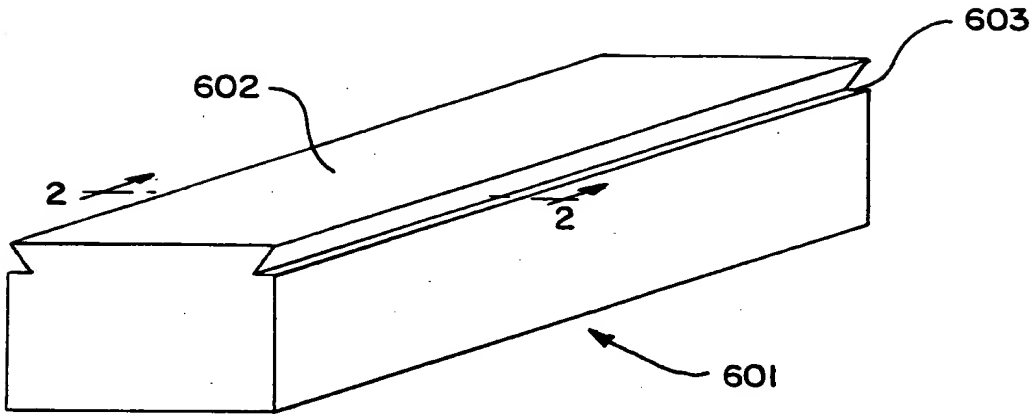

FIG. 2A

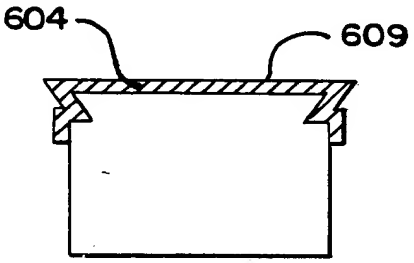

FIG. 2B

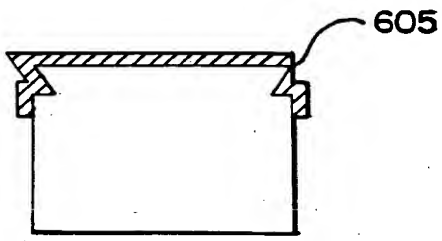

FIG. 2C

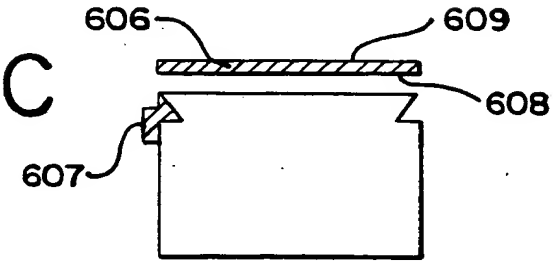

FIG. 3

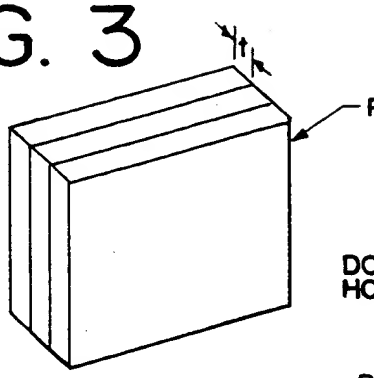

FIG. 3A

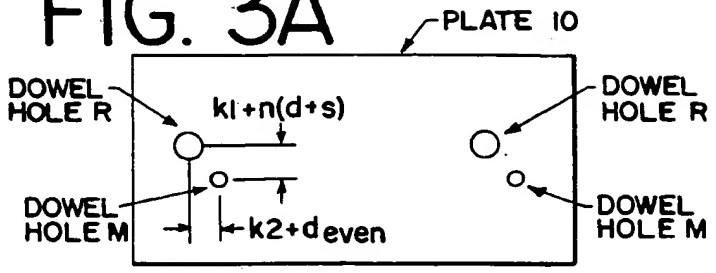

FIG. 4

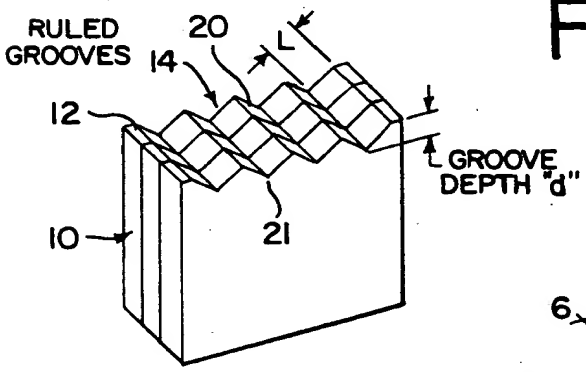

FIG. 5

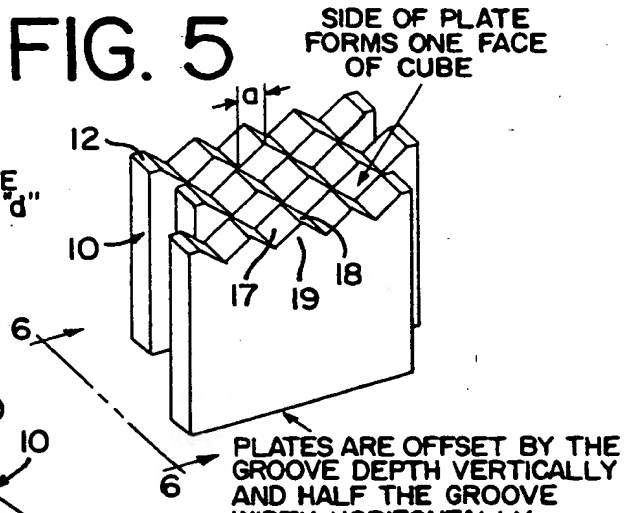

FIG. 6A

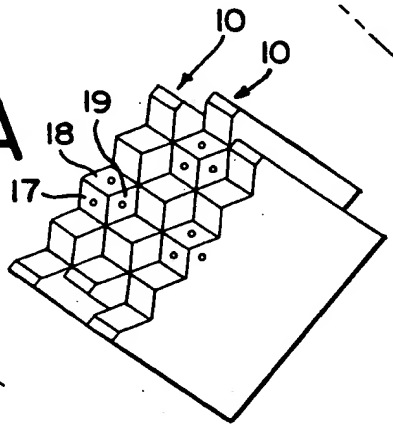

FIG. 6

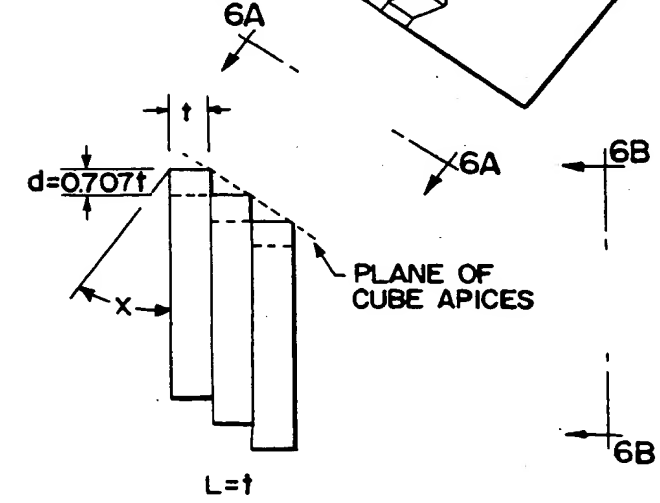

FIG. 6B

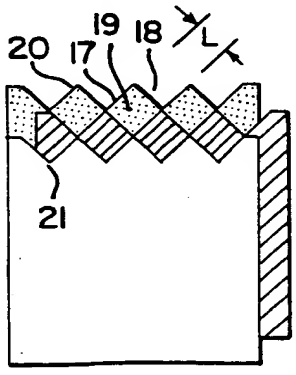

FIG. 7A

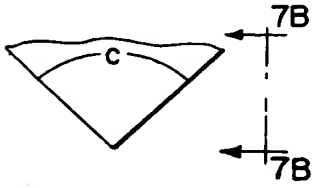

FIG. 7B

FIG. 9

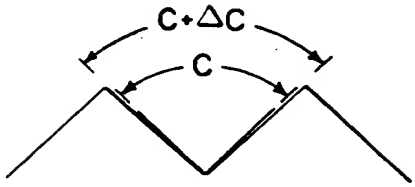

FIG. 8A

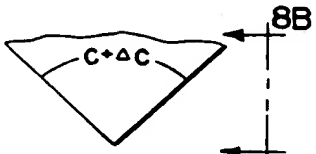

FIG. 8B

TOOL DIRECTION DURING CUTTING

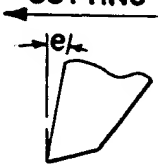

FIG. 10B

PROJECTION PERPENDICULAR TO THE PLANE OF THE CUBE APICES

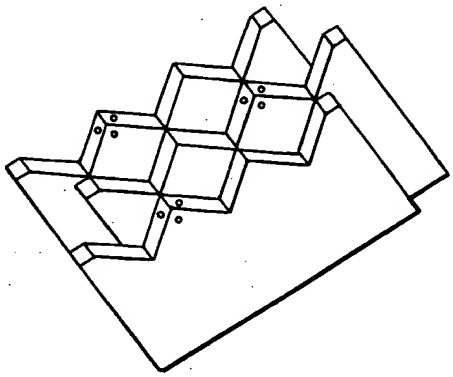

FIG. 10A

PROJECTION ALONG CUBE DIAGONAL

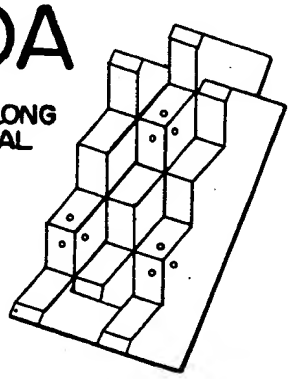

FIG. 10

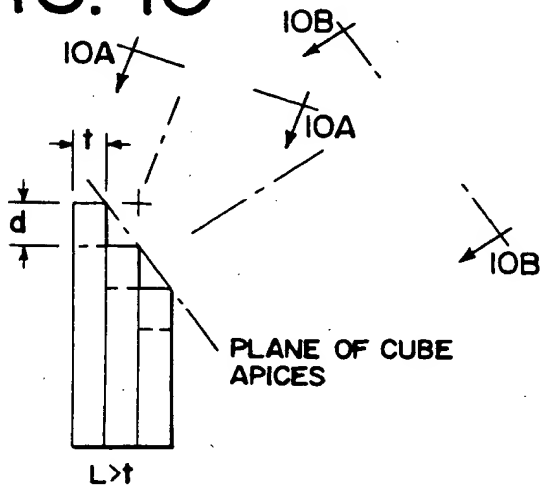

FIG. 10C

PROJECTION PERPENDICULAR TO FACE OF PLATE

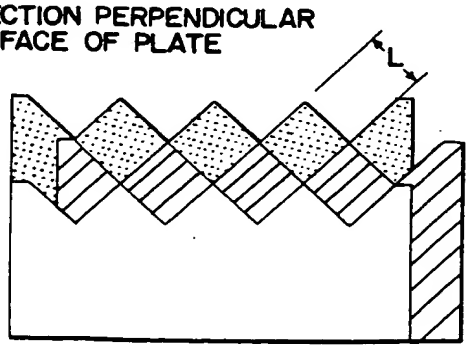

FIG. 11A

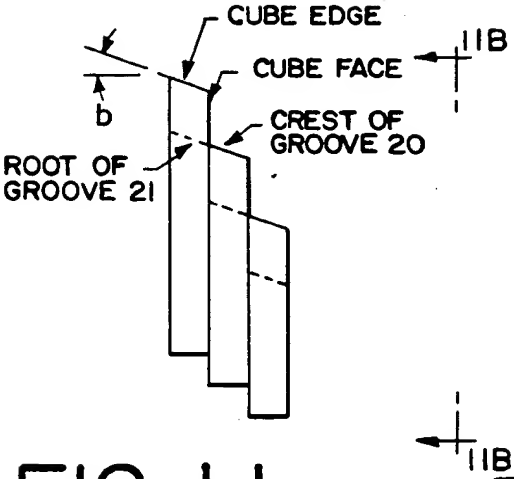

FIG. 11B

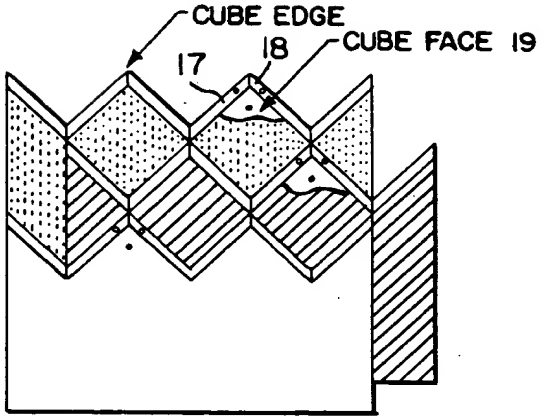

FIG. 11

PLATE ANGLE HIGHLY EXAGGERATED

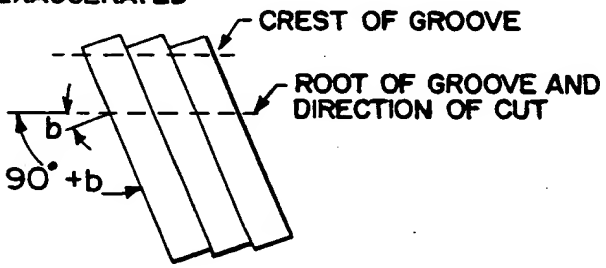

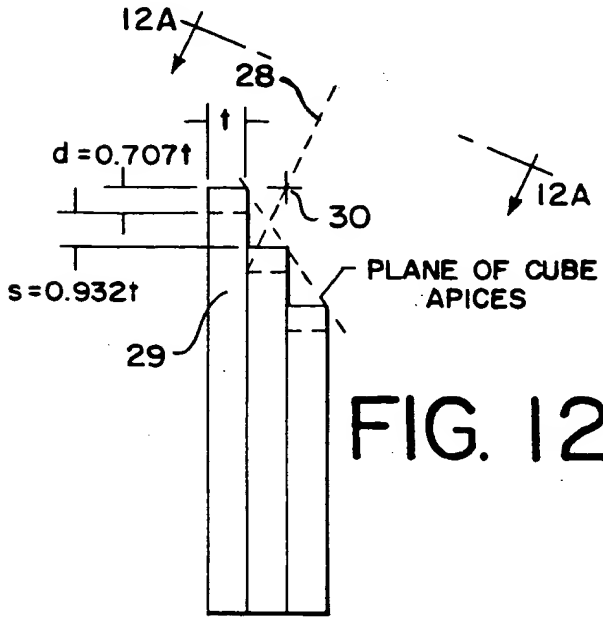

FIG. 12

PLATES DISPLACED SO GROOVE EDGE DOES NOT MEET GROOVE ROOT OF ADJACENT PLATE L=t

FIG. 12A PROJECTION ALONG CUBE DIAGONAL

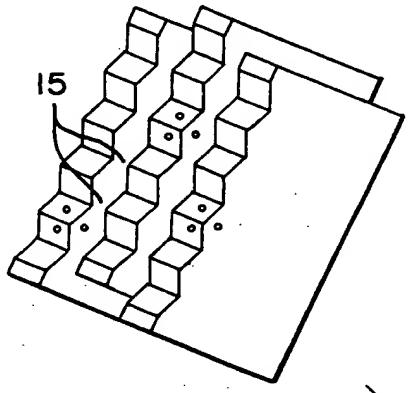

FIG. 12B

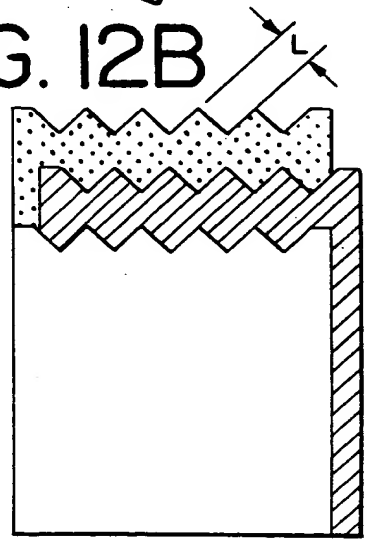

PROJECTION PERPENDICULAR TO FACE PLATE

FIG. 12C

INTERRELATIONSHIP OF
d, s, t, I AND I'
FOR NEGATIVE VALUES OF I

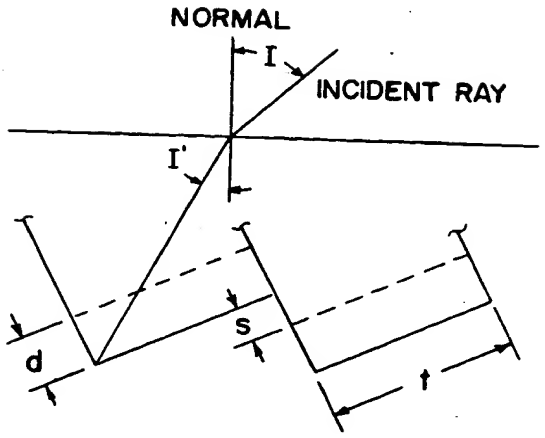

FIG. 12D

INTERRELATIONSHIP OF
d, s, t, I AND I'
FOR POSITIVE VALUES OF I

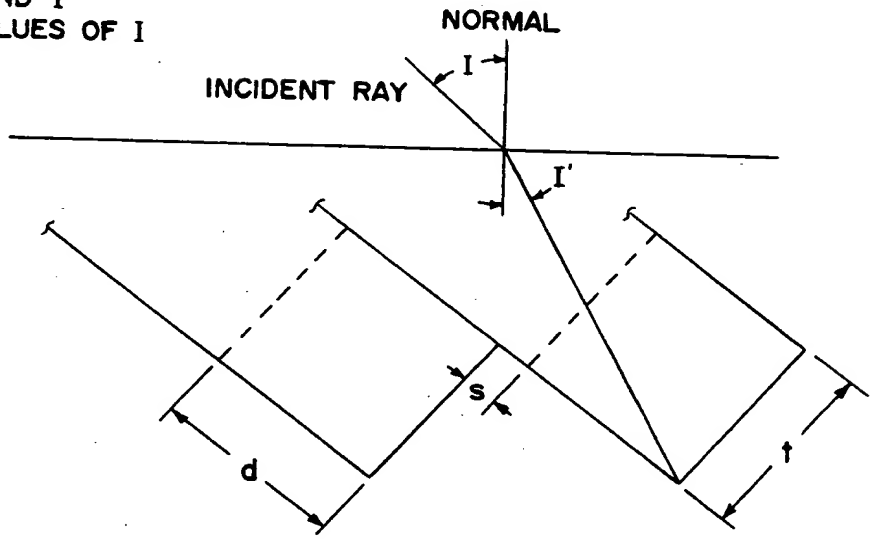

FIG. 13

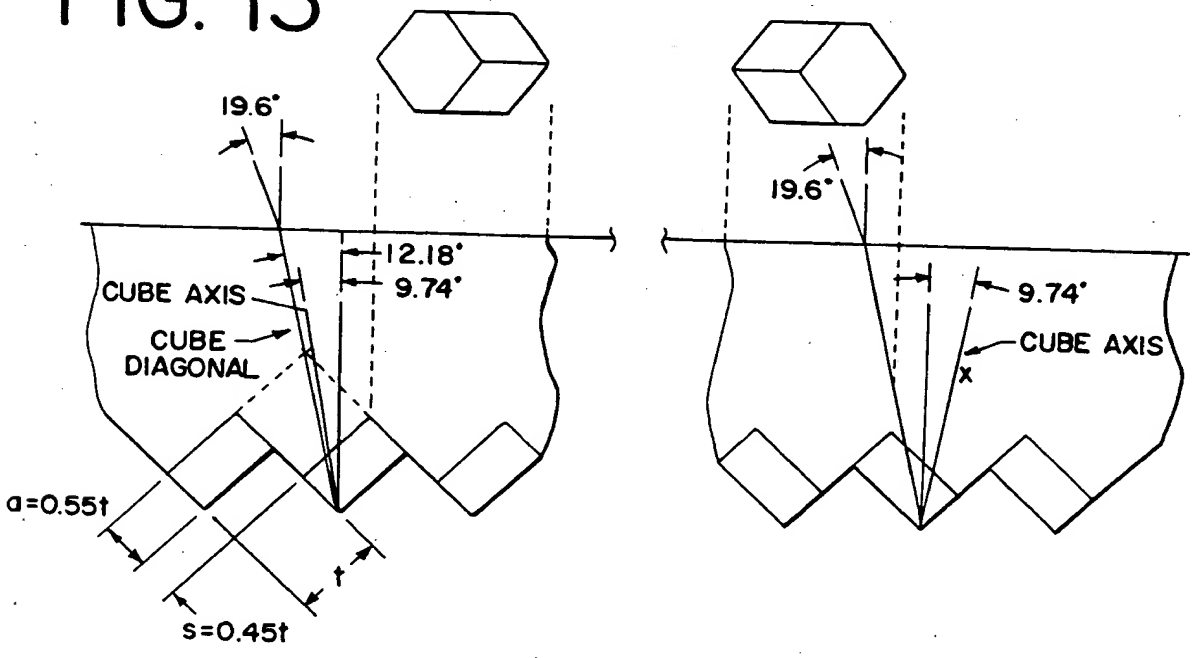

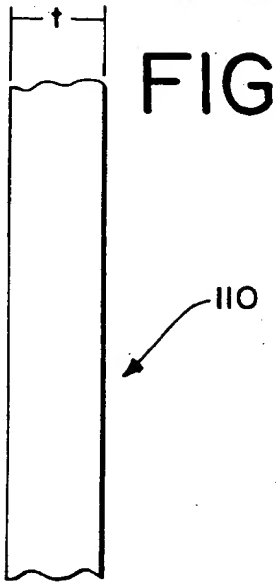

FIG. 14A

FIG. 14B

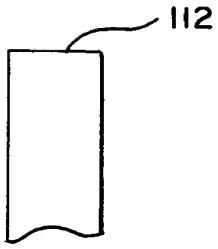

FIG. 15

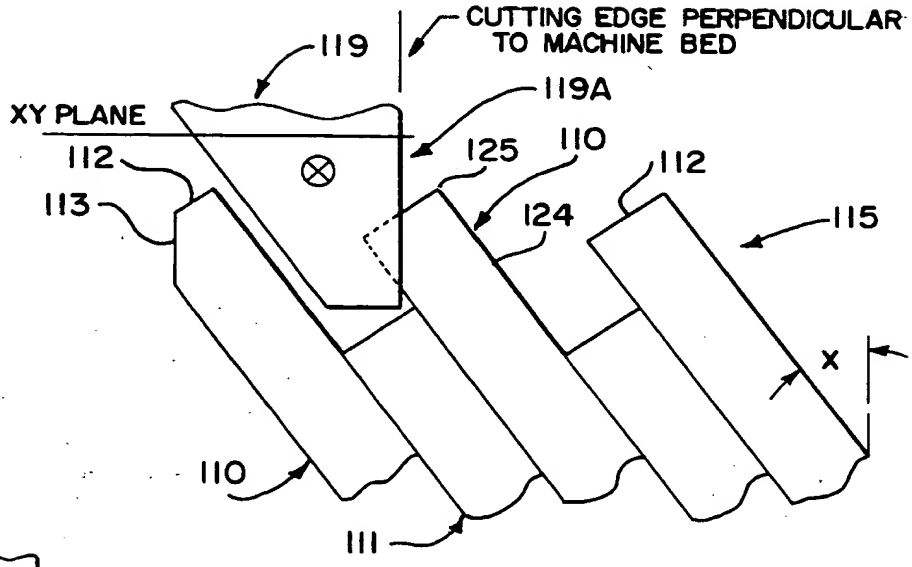

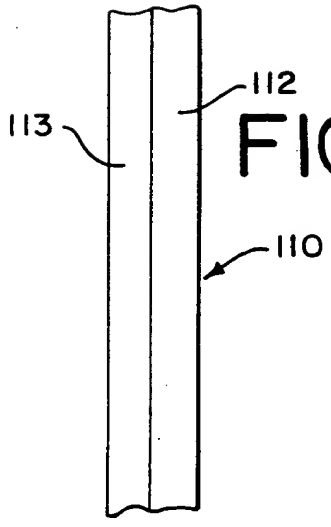

FIG. 16A

FIG. 16B

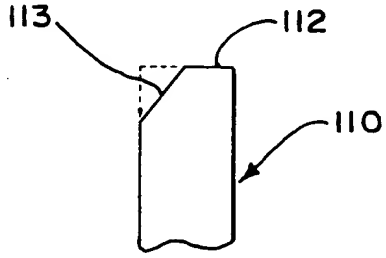

FIG. 17

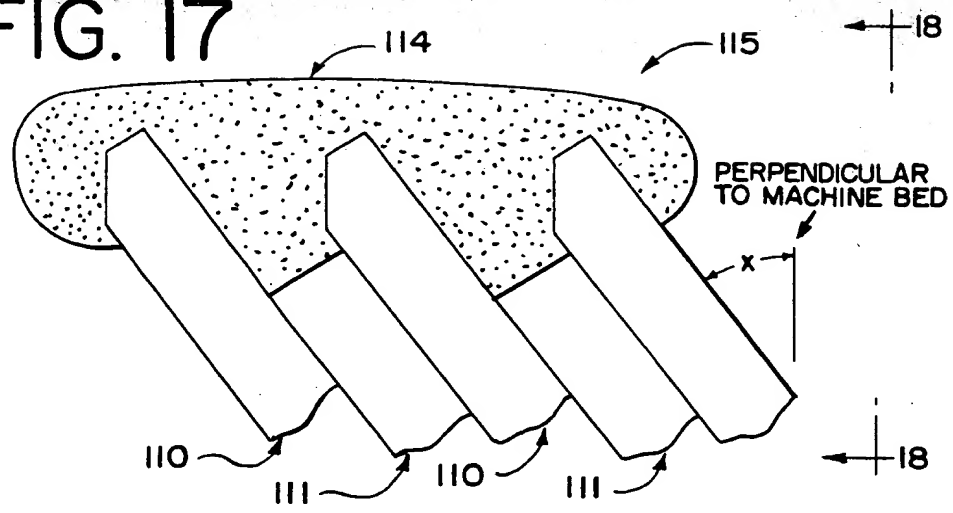

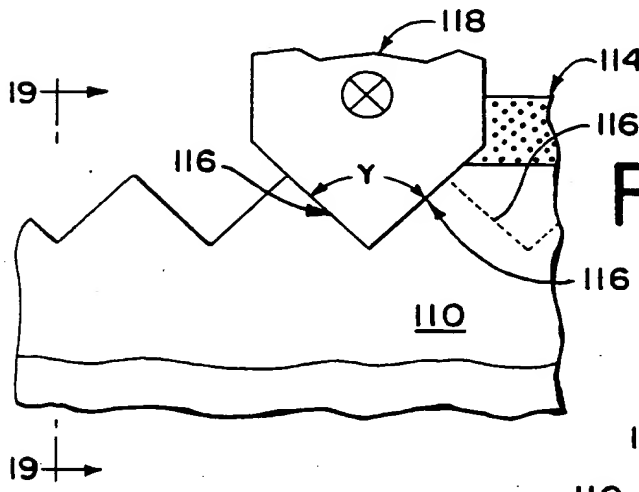

FIG. 18

FIG. 21

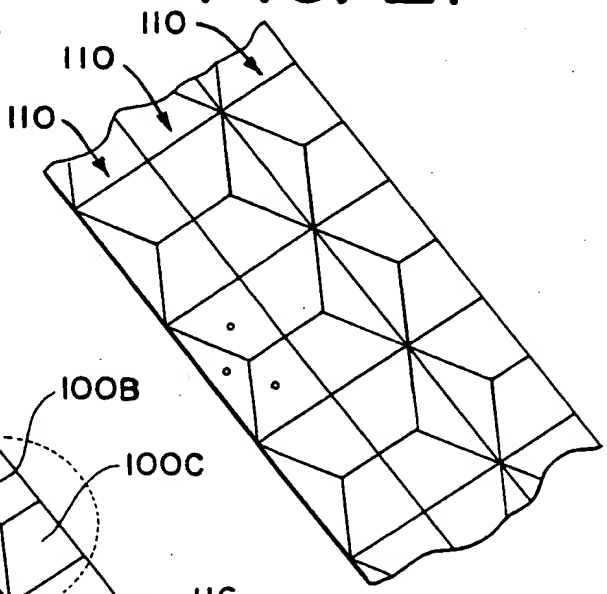

FIG. 20

FIG. 19

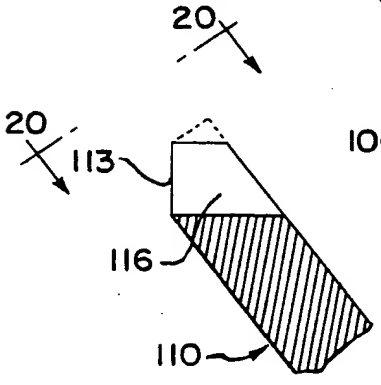

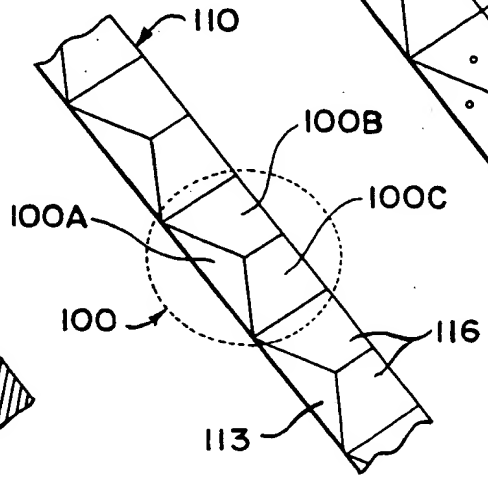

FIG. 22A

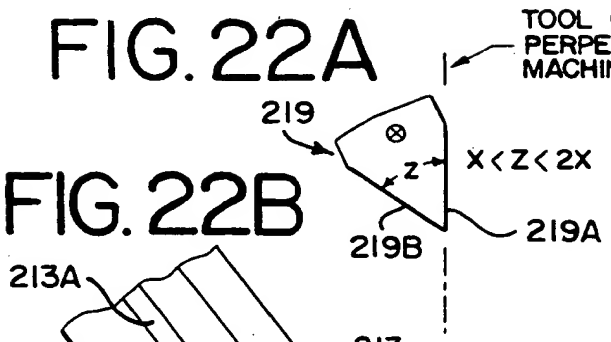

FIG. 22B

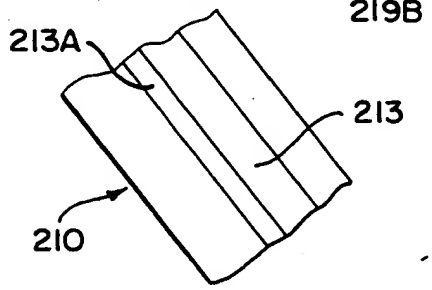

FIG. 22C

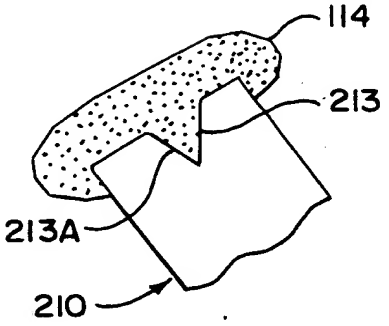

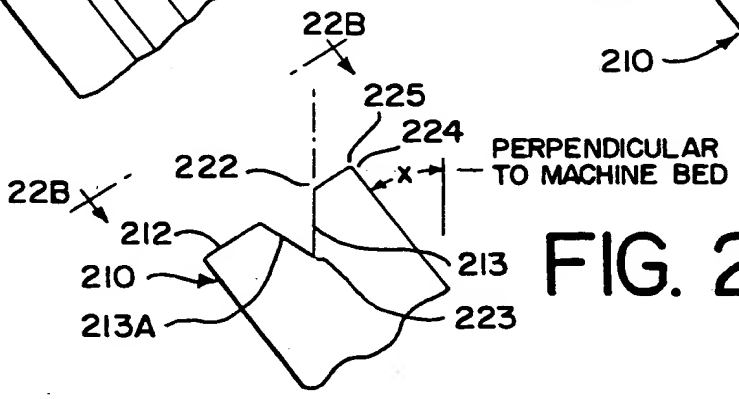

FIG. 22

FIG. 23

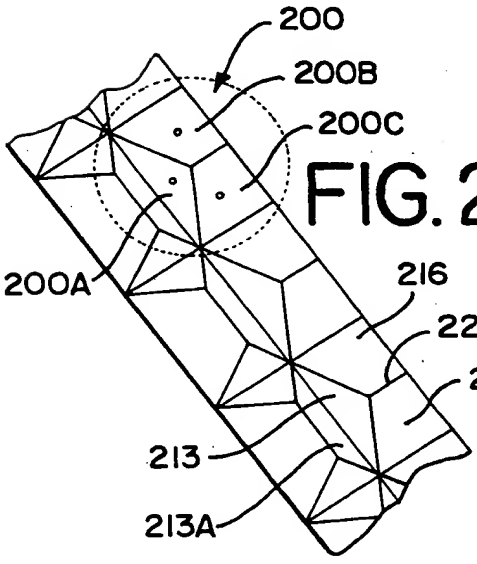

FIG. 23B

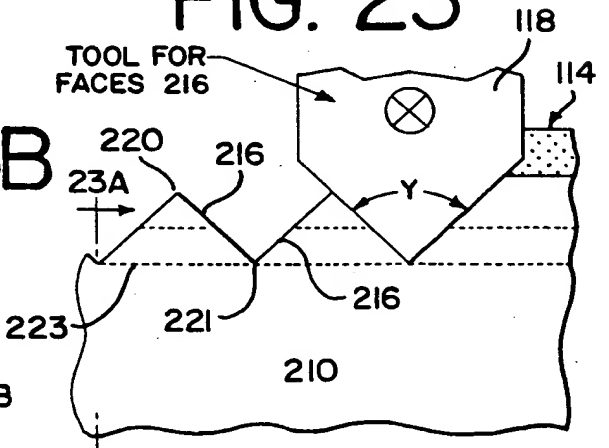

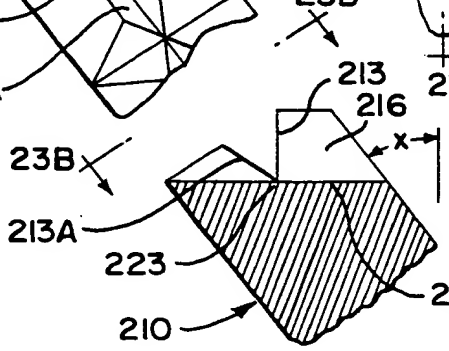

FIG. 23A

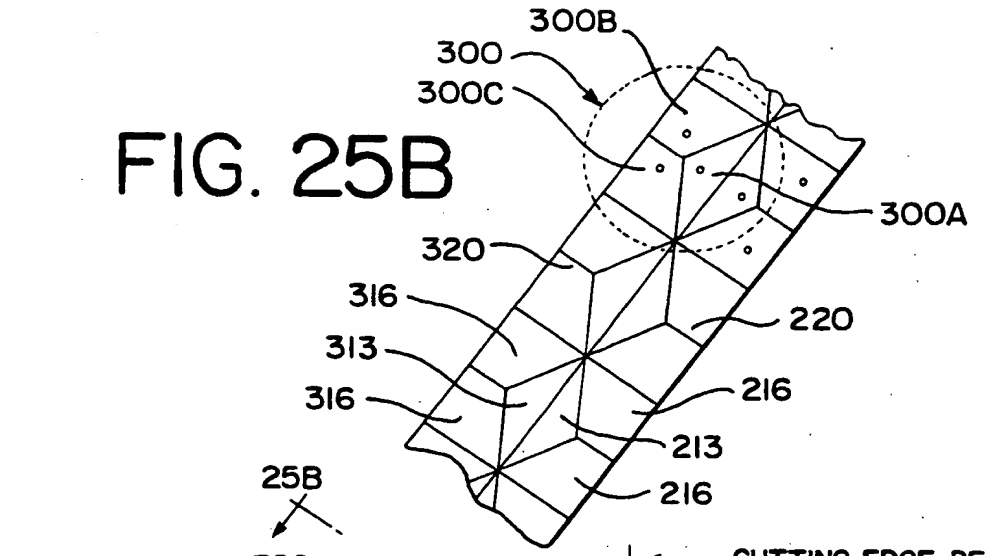

FIG. 25B

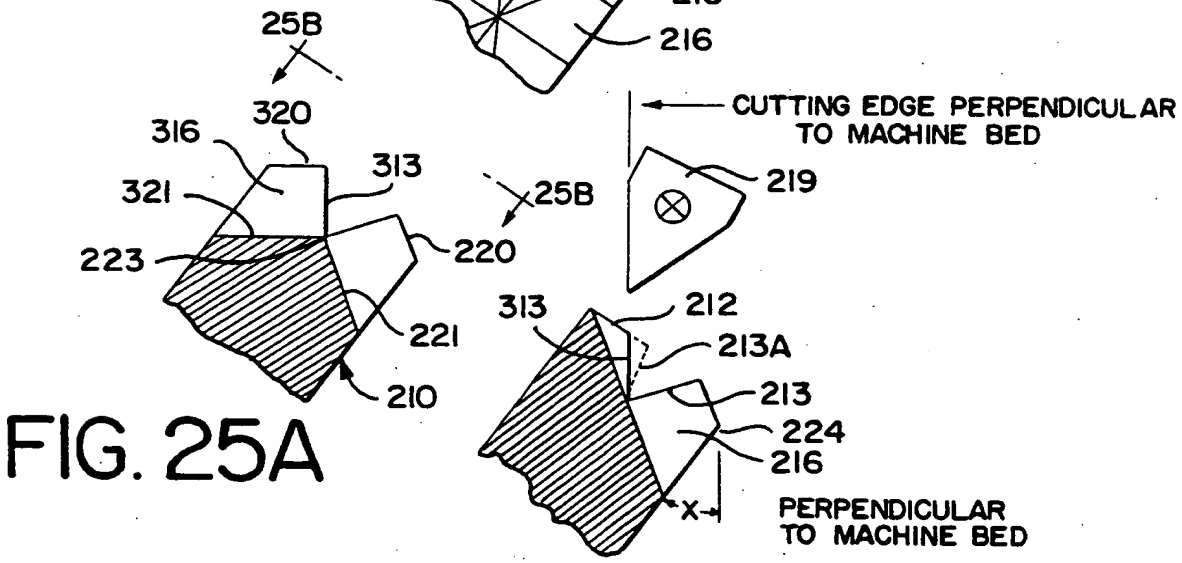

FIG. 25A

FIG. 24

FIG. 25

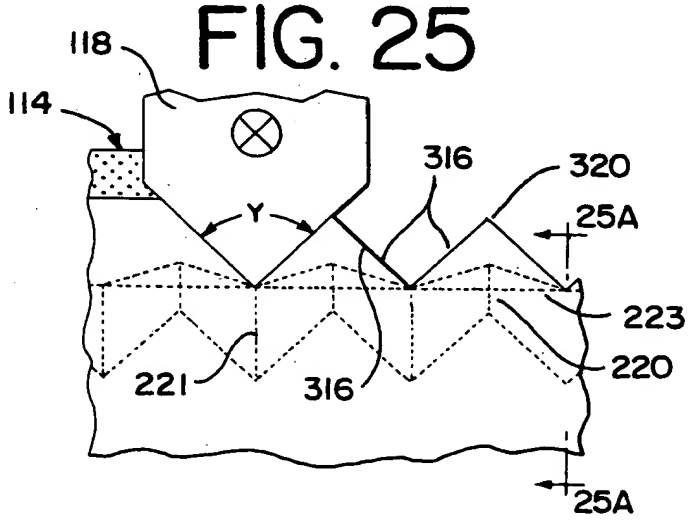

FIG. 26

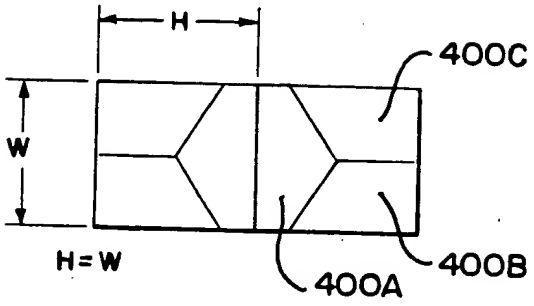

FIG. 27B

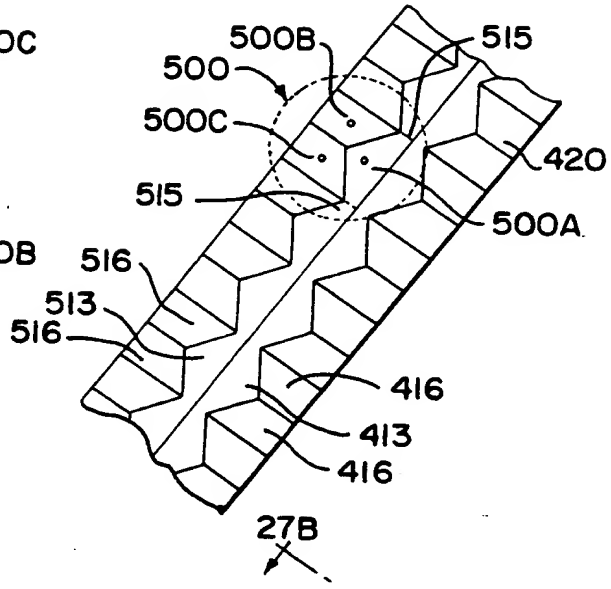

FIG. 27

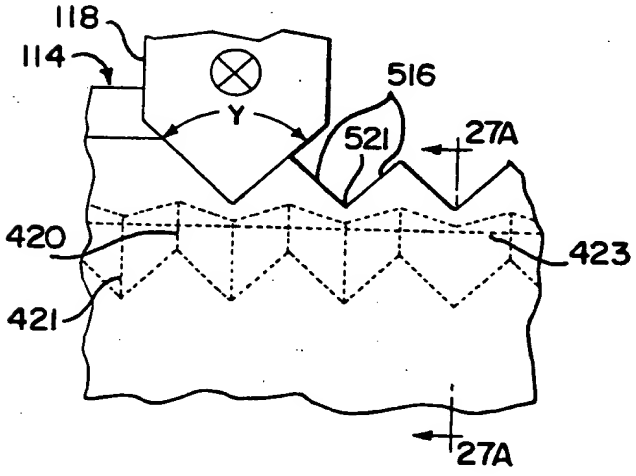

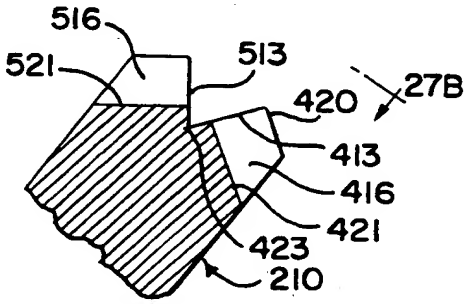

FIG. 27A

FIG. 27C

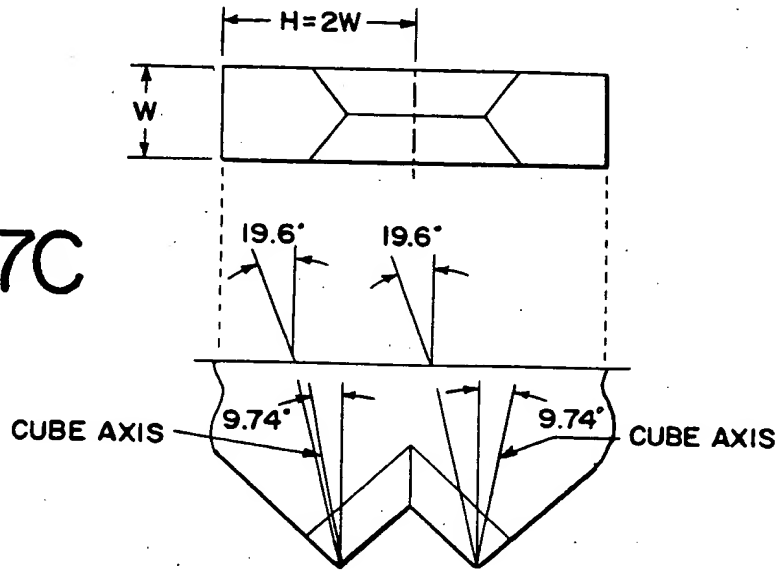

FIG. 28

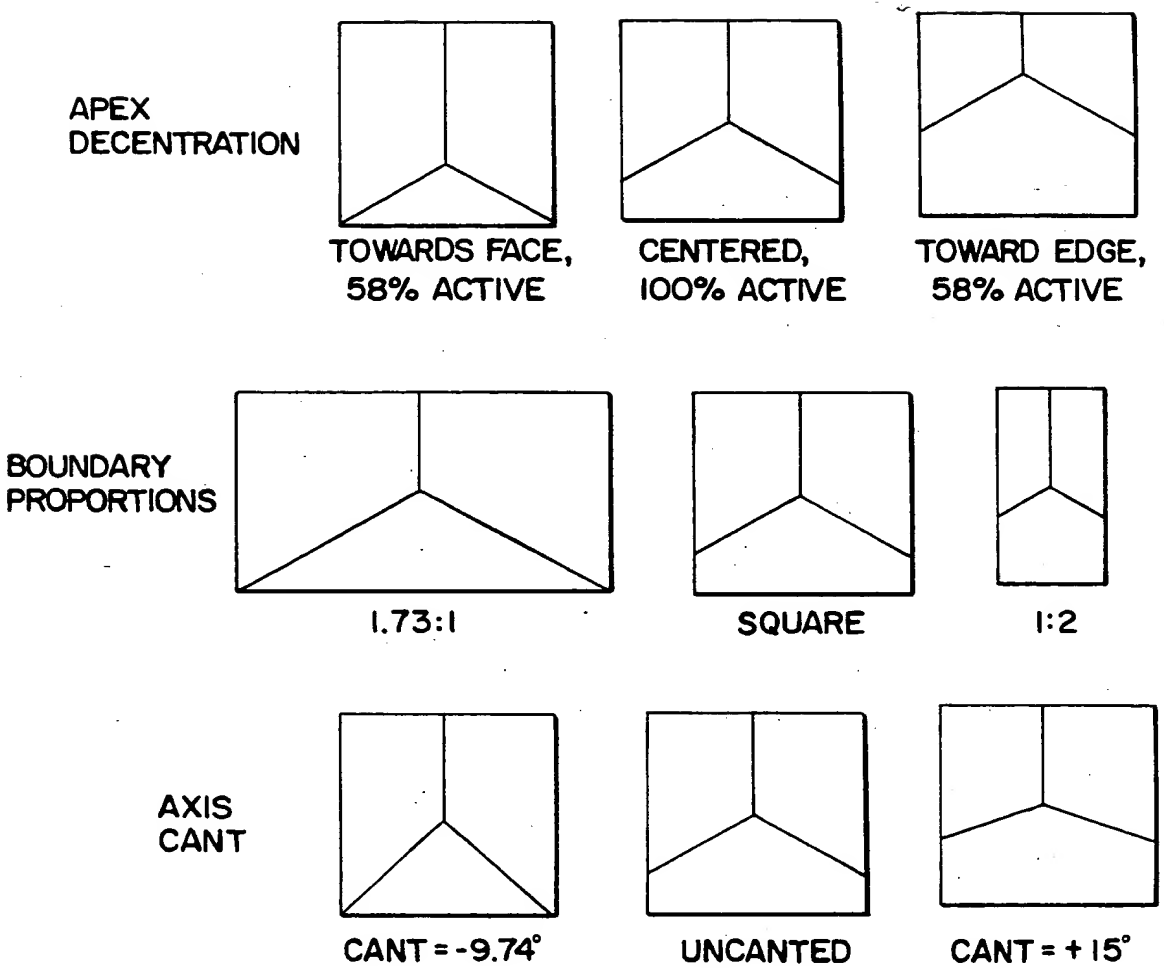
APEX
DECENTRATION
TOWARDS FACE,
58% ACTIVE
CENTERED,
100% ACTIVE
TOWARD EDGE,
58% ACTIVE
BOUNDARY
PROPORTIONS
1.73:1
SQUARE
1:2
AXIS
CANT
CANT = -9.74°
UNCANTED
CANT = + 15°

FIG. 29A

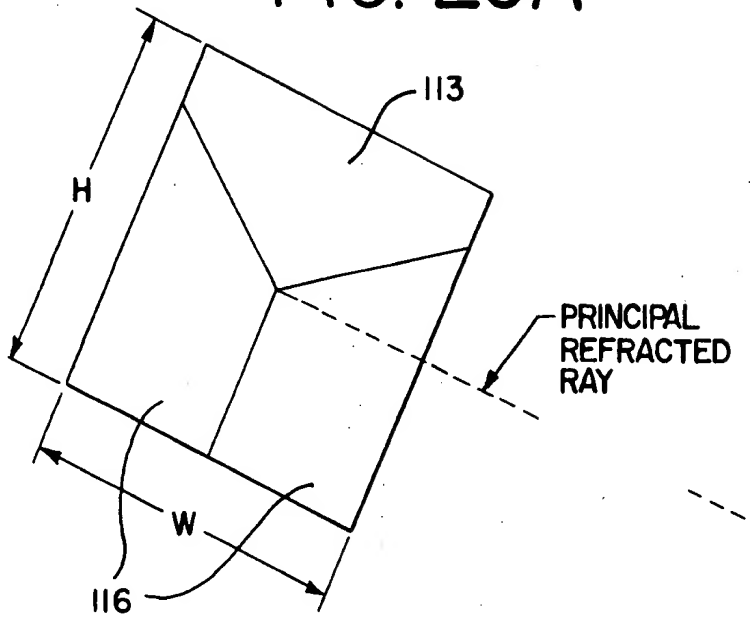

FIG. 29

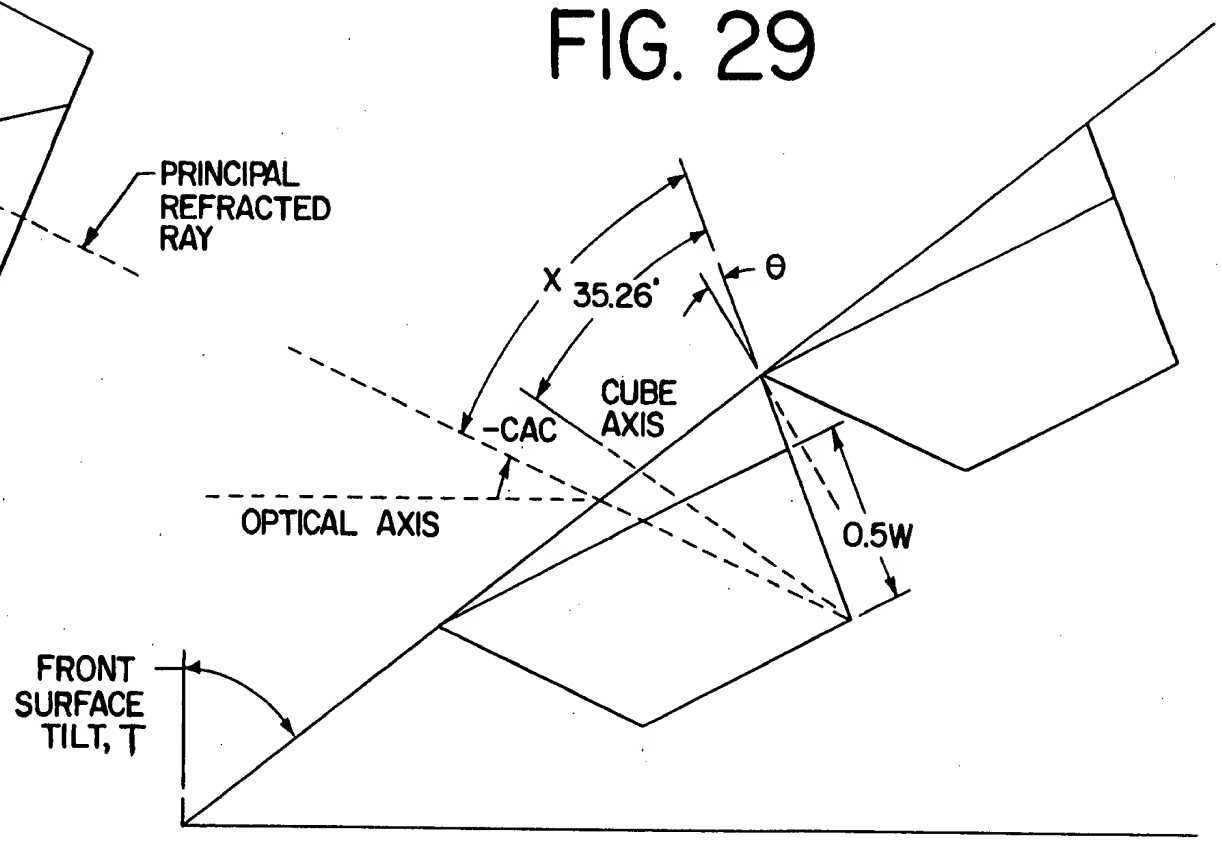

FIG. 30

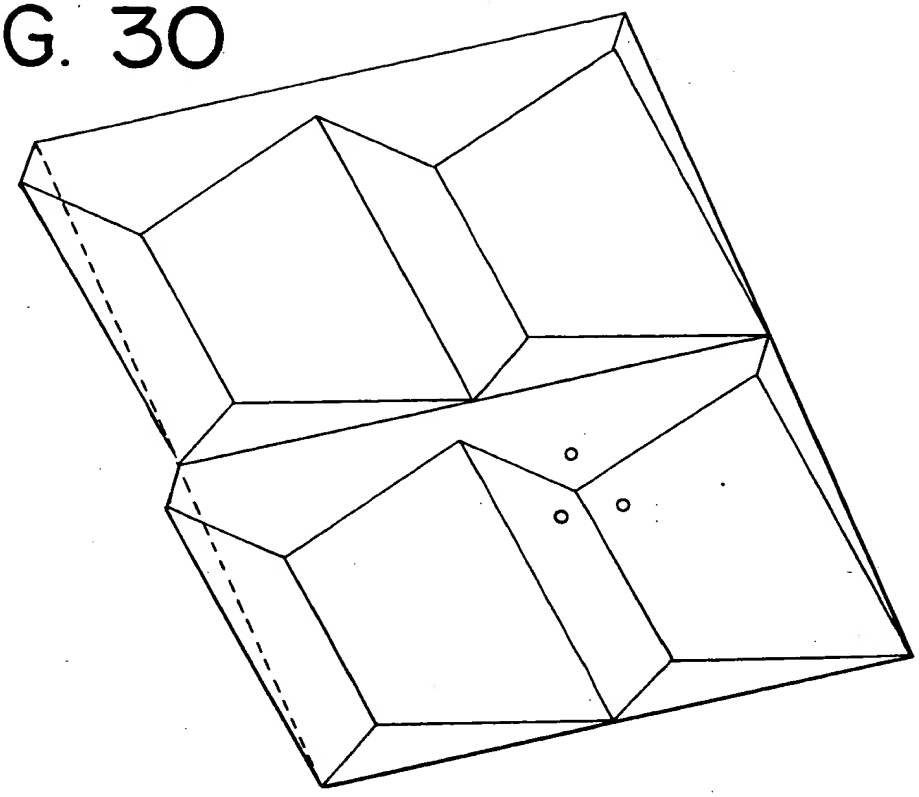

FIG. 31

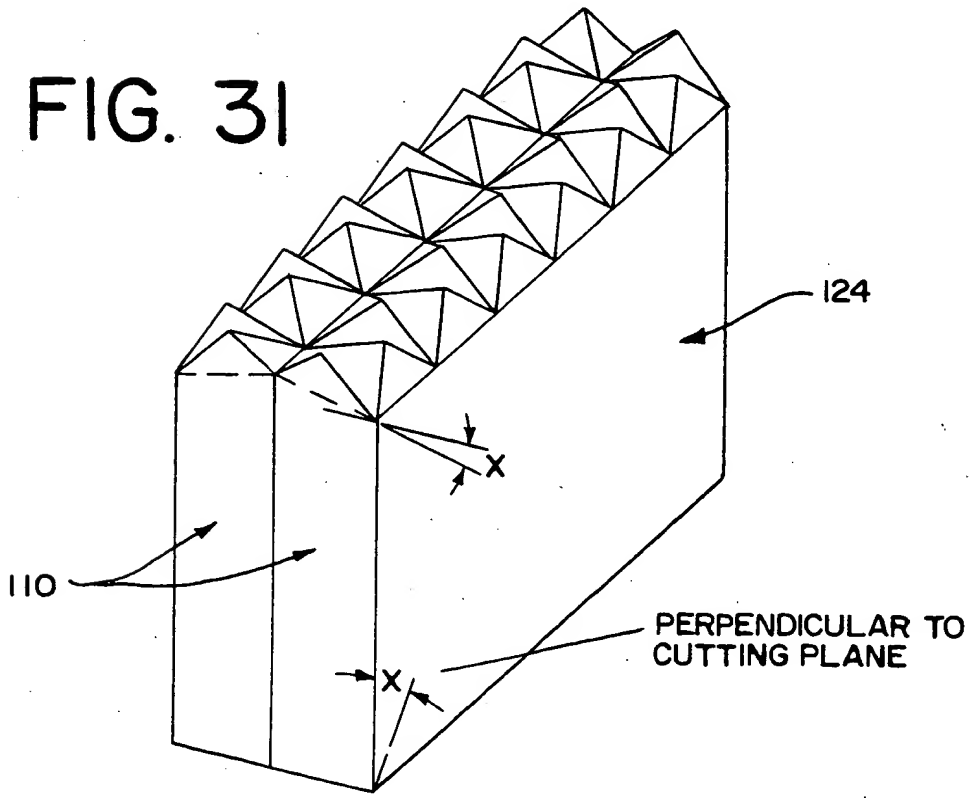

FIG. 32

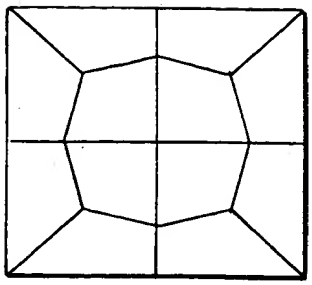

FIG. 33

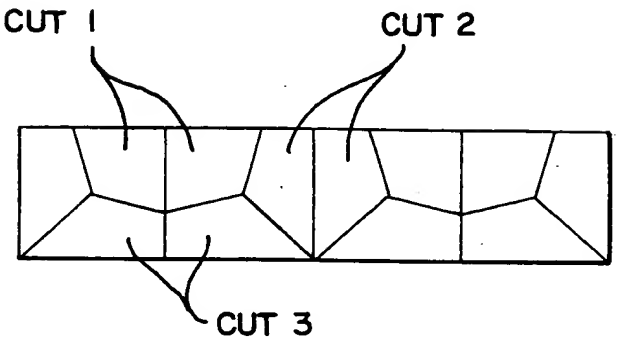

FIG. 34A

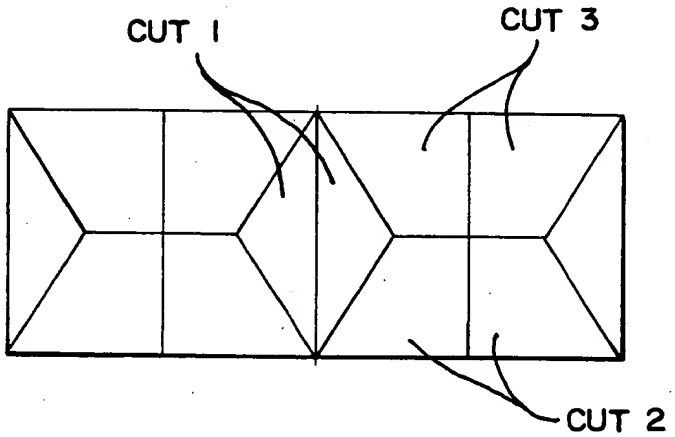

FIG. 34B

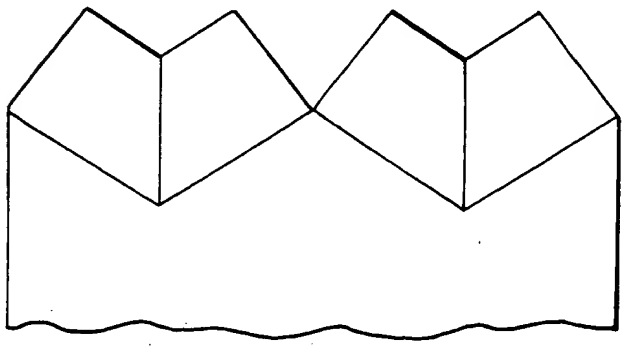

FIG. 35 ARRAY OF PENTA-FACE HEXAGONAL CUBES SHOWING A PLATE HIGHLIGHTED

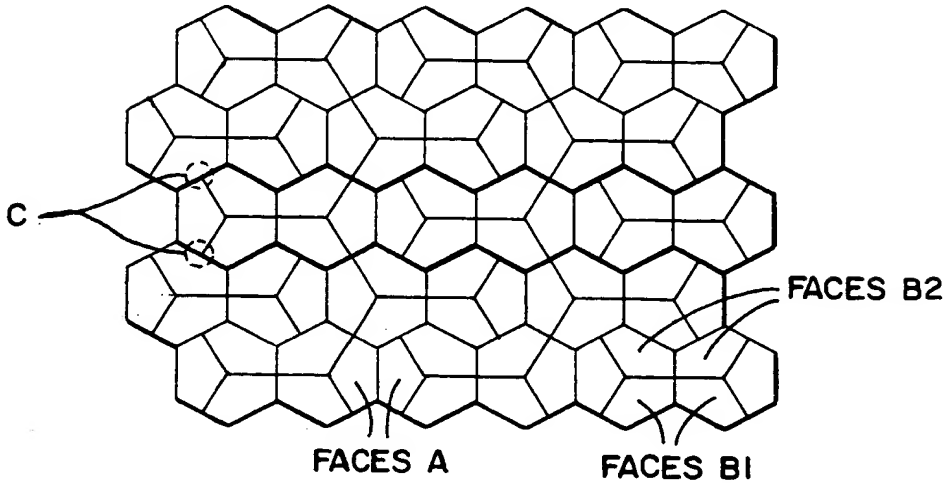

FIG. 36

ARRAY OF PENTAGONAL CUBES WITH +8.7 AXIS TILT AND 89.8 AREA EFFICIENCY

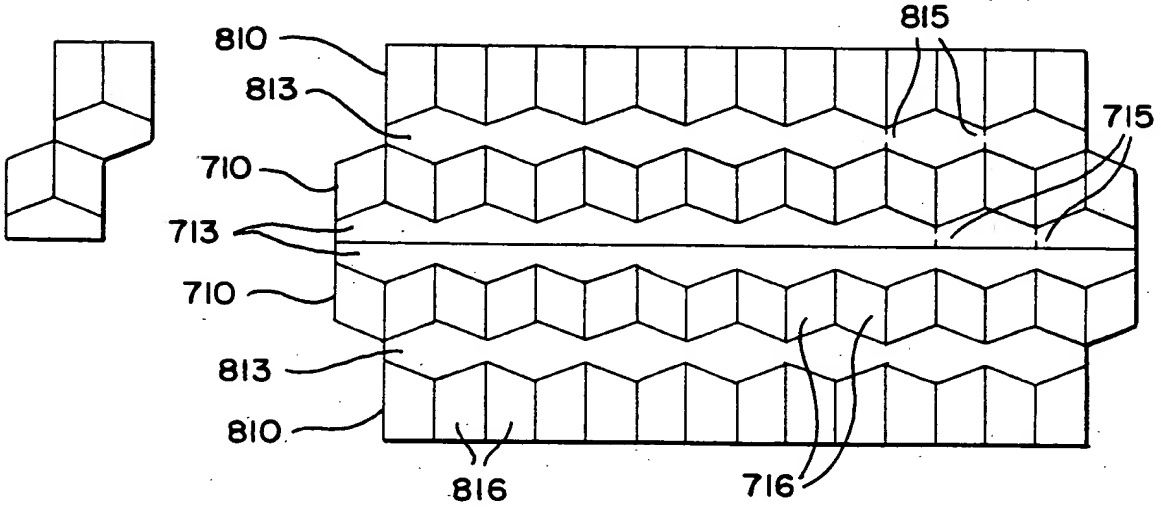

FIG. 36A

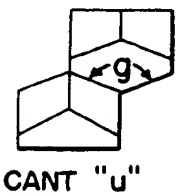

$$g = 2\arctan\frac{\sqrt{3}\cos(v-u)}{\cos(v)-\sqrt{2}\sin(v)}$$

FIG. 37

PERFORMANCE OF SIMPLEST HEXBLADE ARRAY (d/t=.7071, s/t=0, NOT PAIRED)
FORMED IN MATERIALS OF DIFFERENT REFRACTIVE INDICES

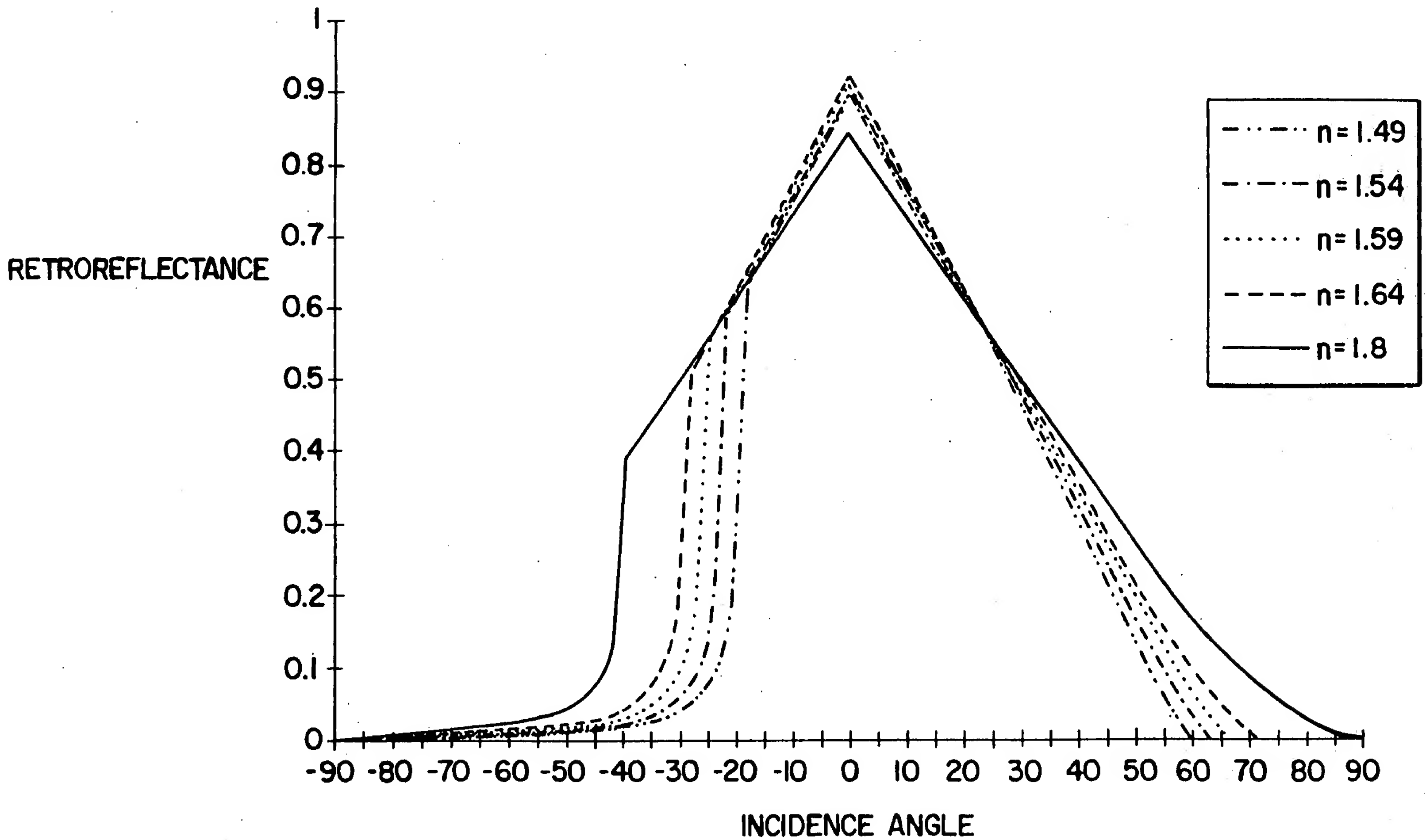

FIG. 38

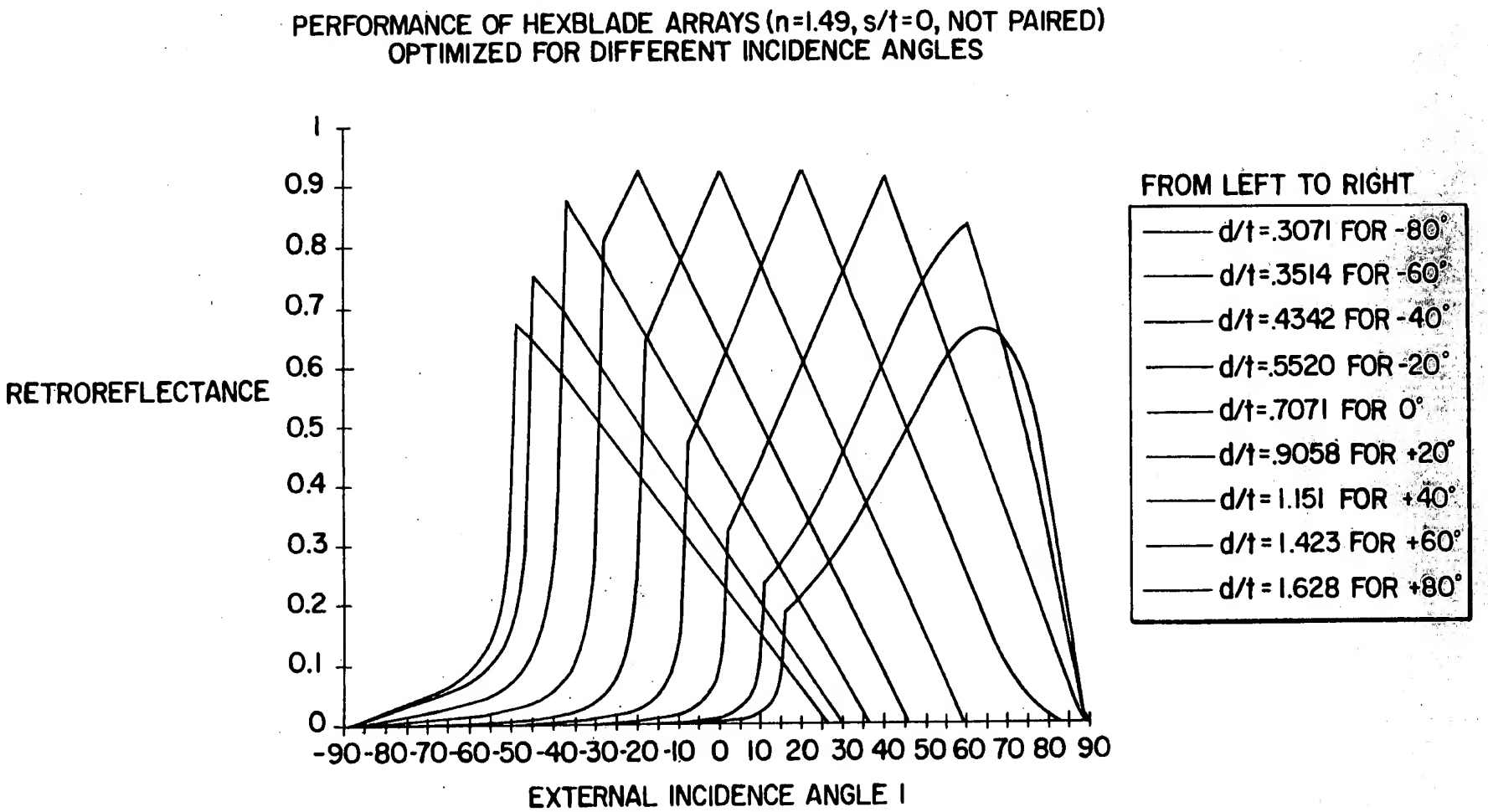
PERFORMANCE OF HEXBLADE ARRAYS (n=1.49, s/t=0, NOT PAIRED)
OPTIMIZED FOR DIFFERENT INCIDENCE ANGLES
RETROREFLECTANCE
1
0.9
0.8
0.7
0.6
0.5
0.4
0.3
0.2
0.1
0
-90 -80 -70 -60 -50 -40 -30 -20 -10 0 10 20 30 40 50 60 70 80 90
EXTERNAL INCIDENCE ANGLE I
FROM LEFT TO RIGHT
d/t=.3071 FOR -80°
d/t=.3514 FOR -60°
d/t=.4342 FOR -40°
d/t=.5520 FOR -20°
d/t=.7071 FOR 0°
d/t=.9058 FOR +20°
d/t=1.151 FOR +40°
d/t=1.423 FOR +60°
d/t=1.628 FOR +80°

FIG. 39

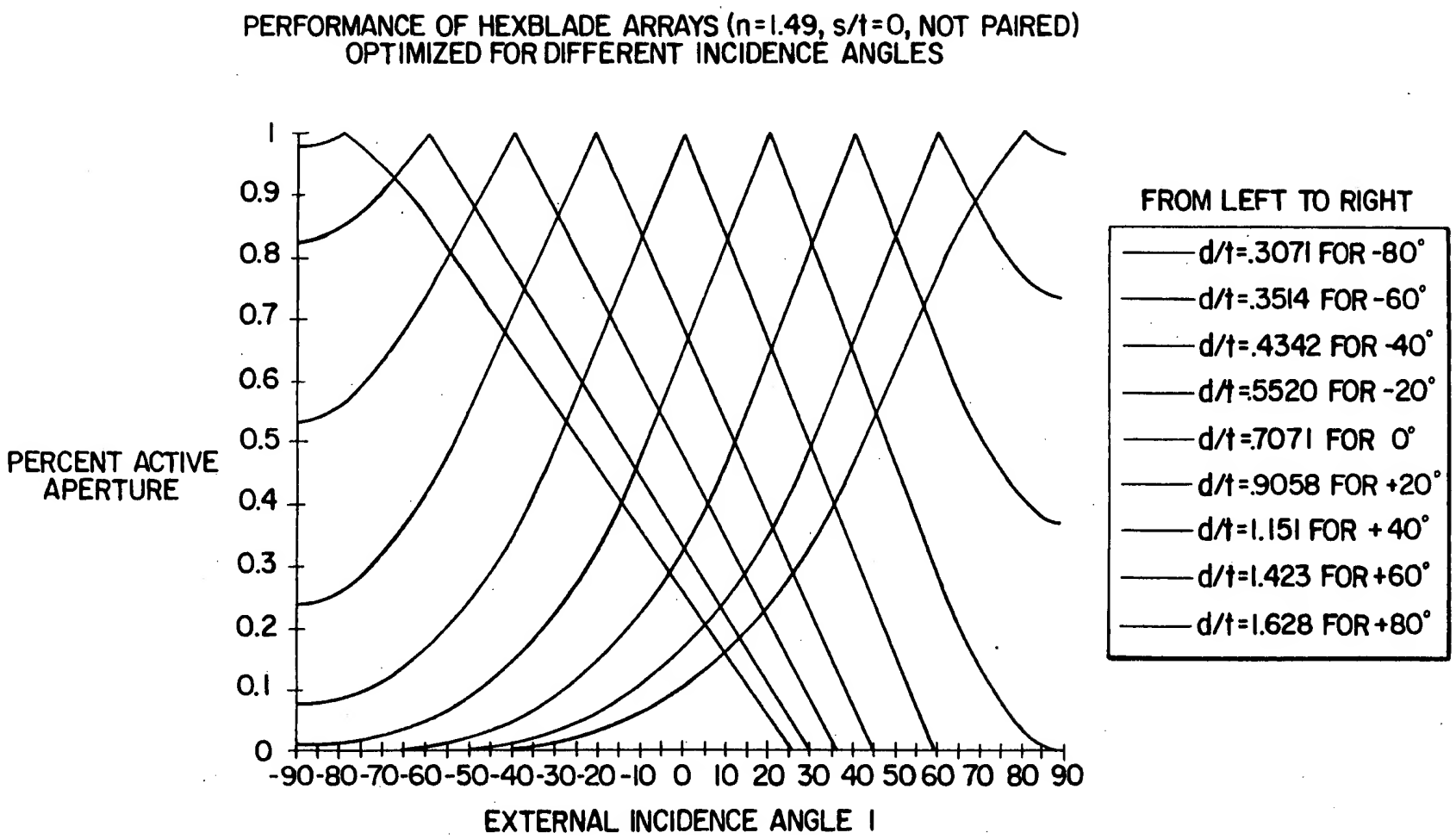

FIG. 40

RECTANGLE AND HEXAGON MICROCUBES OF EXAMPLE I (REFRACTIVE INDEX = 1.59)

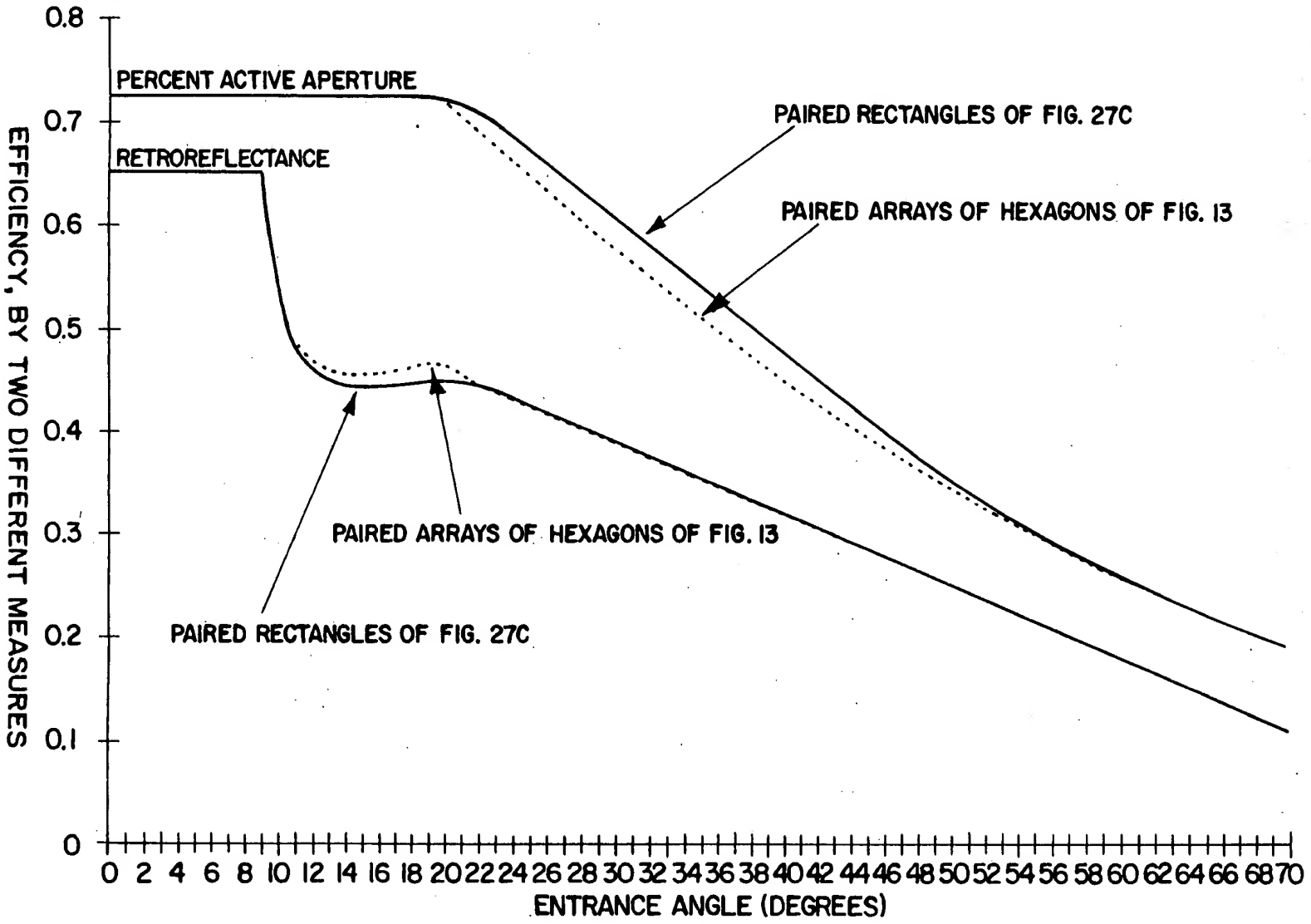

FIG. 41

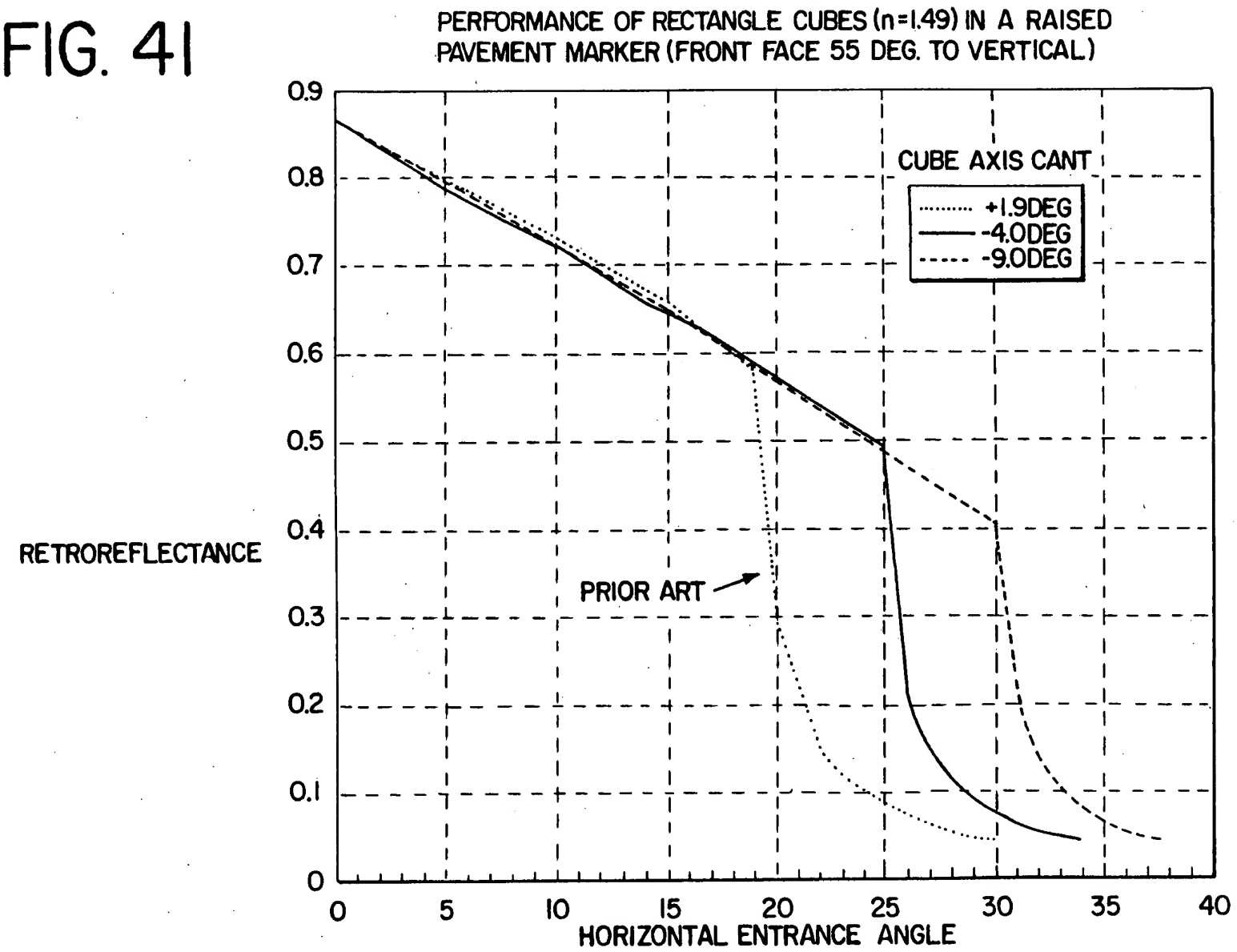
PERFORMANCE OF RECTANGLE CUBES (n=1.49) IN A RAISED PAVEMENT MARKER (FRONT FACE 55 DEG. TO VERTICAL)
RETROREFLECTANCE
0.9
0.8
0.7
0.6
0.5
0.4
0.3
0.2
0.1
0
CUBE AXIS CANT
+1.9DEG
-4.0DEG
-9.0DEG
PRIOR ART
0
5
10
15
20
25
30
35
40
HORIZONTAL ENTRANCE ANGLE

FIG. 42A

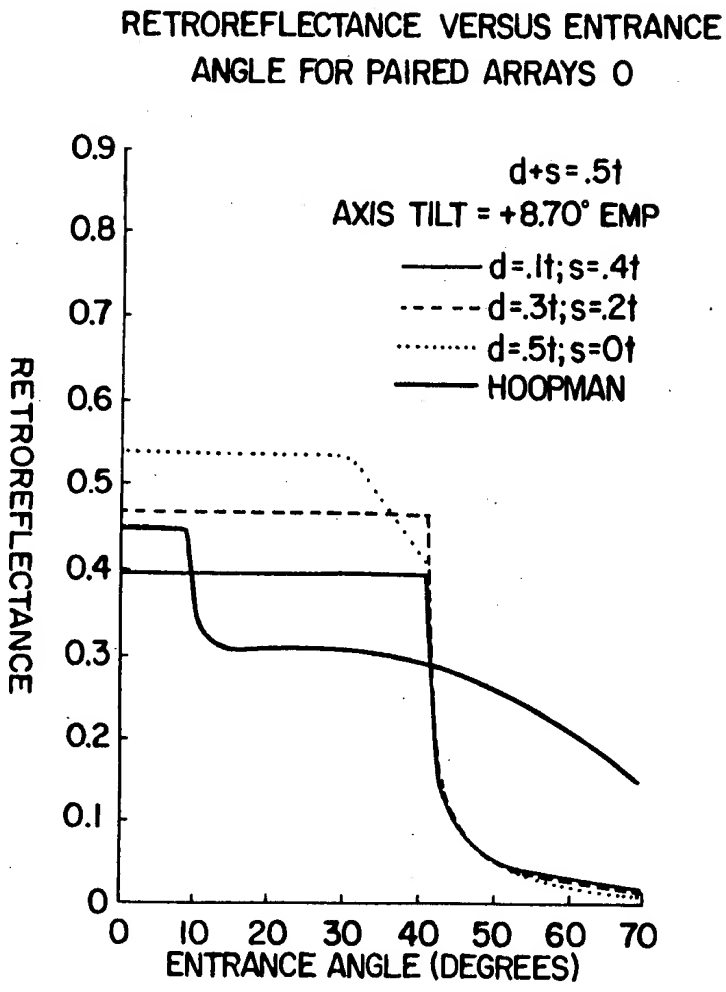

FIG. 42B

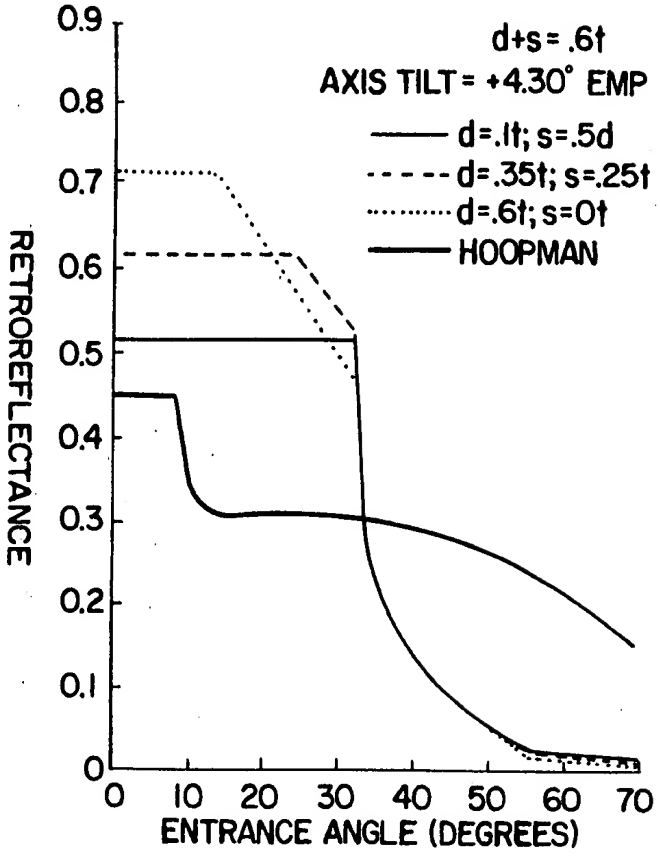

FIG. 42C

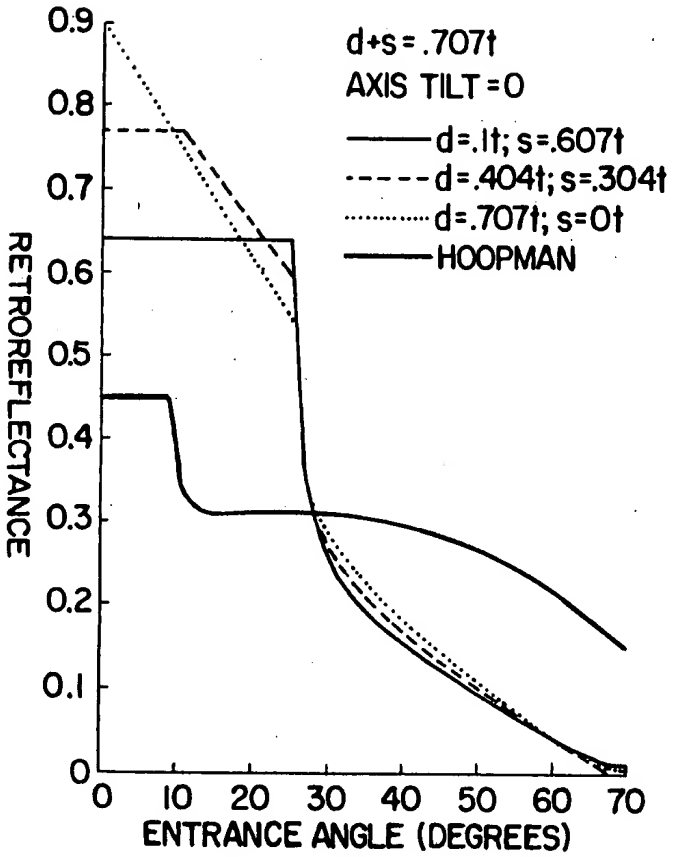

FIG. 42D

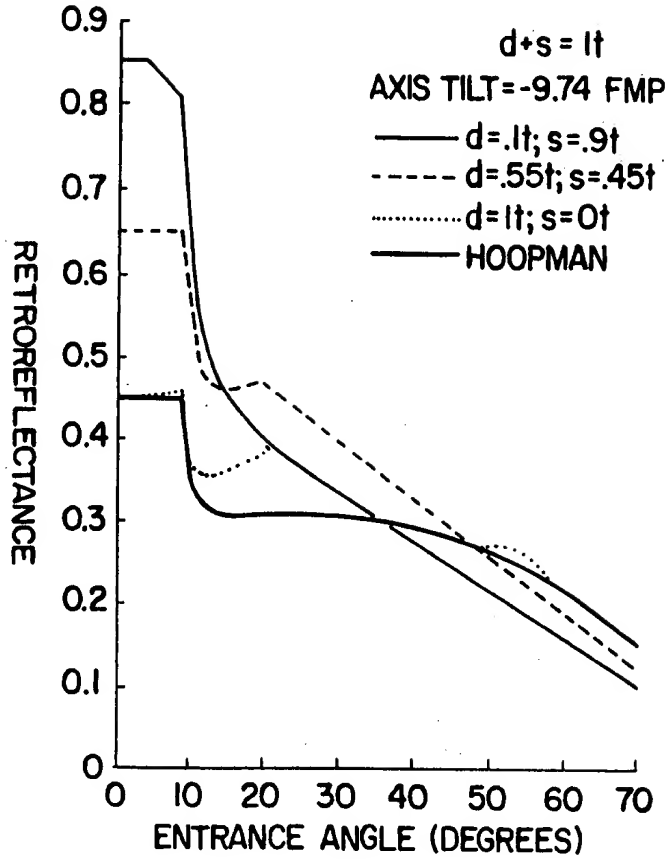

FIG. 42E

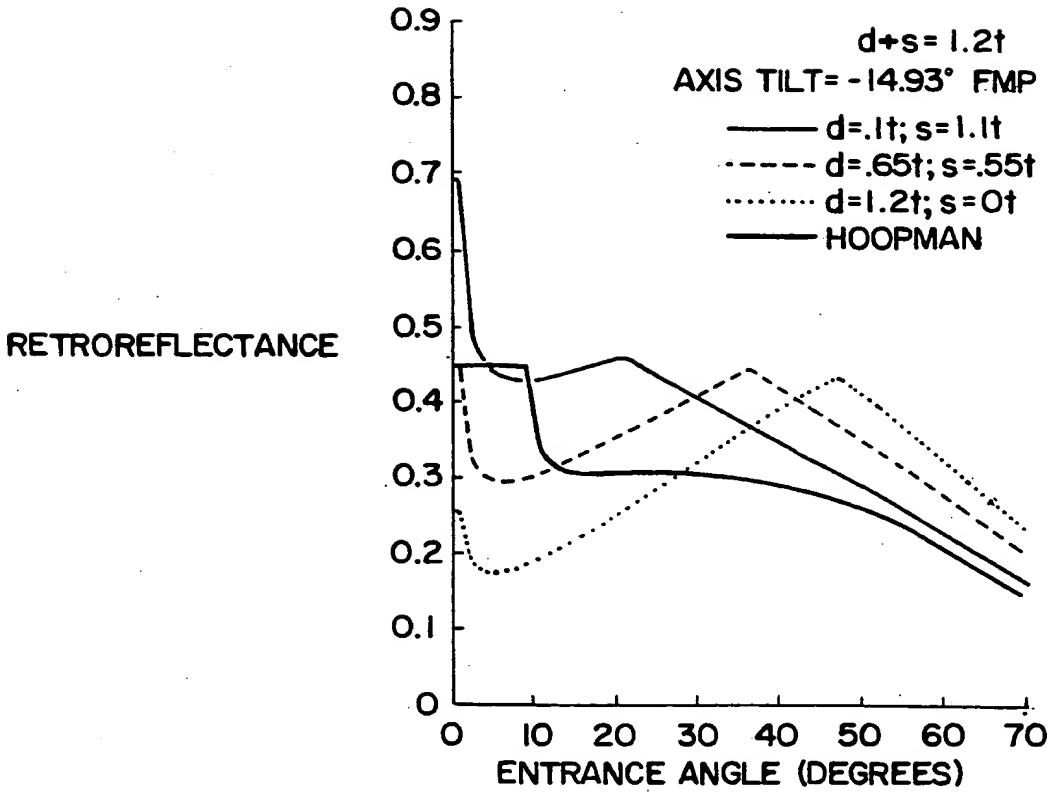
RETROREFLECTANCE
0.9
0.8
0.7
0.6
0.5
0.4
0.3
0.2
0.1
0
0
10
20
30
40
50
60
70
ENTRANCE ANGLE (DEGREES)
d+s= 1.2t
AXIS TILT= -14.93° FMP
d=.1t; s=1.1t
d=.65t; s=.55t
d=1.2t; s=0t
HOOPMAN

FIG. 43

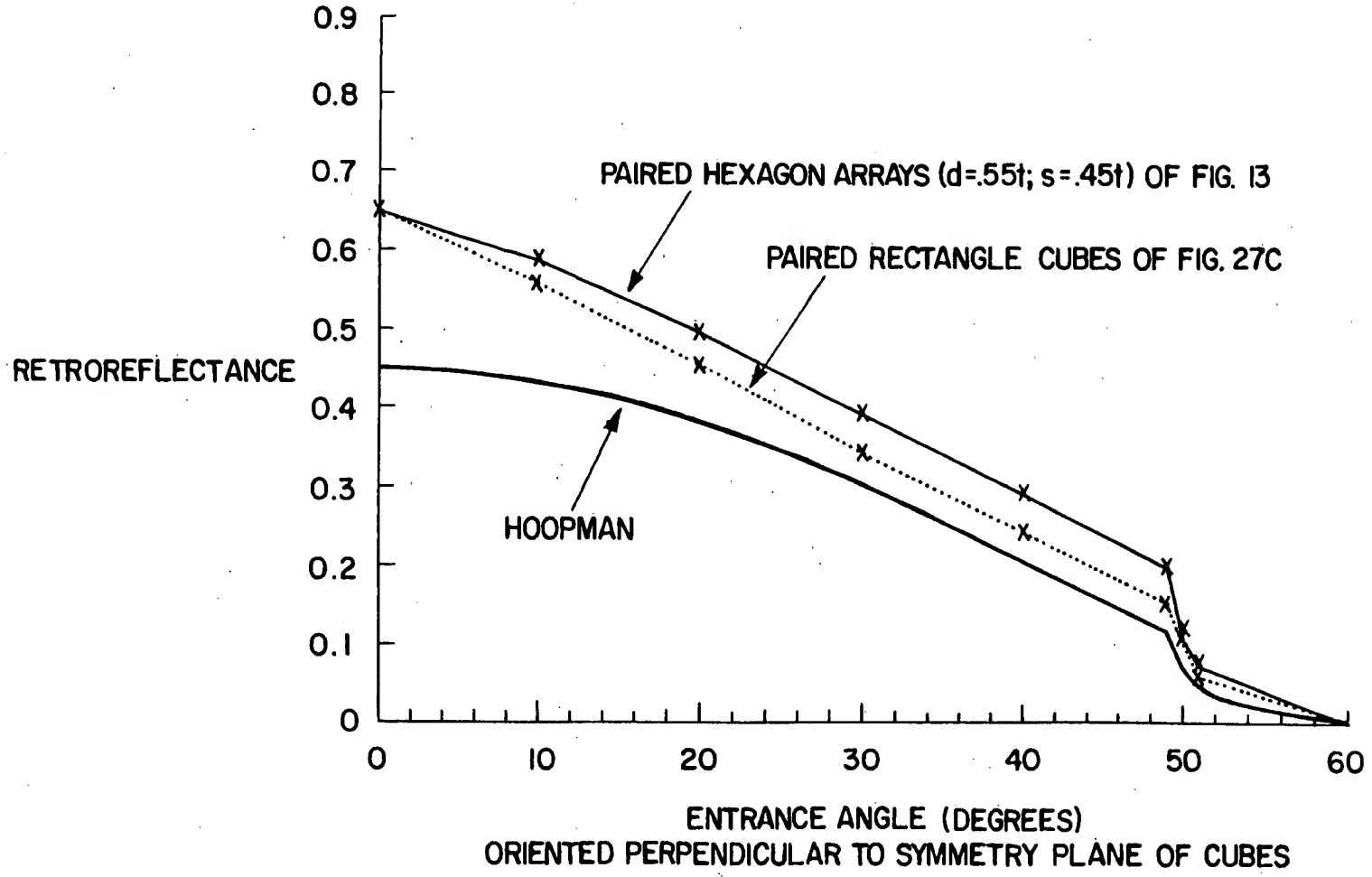

FIG. 44

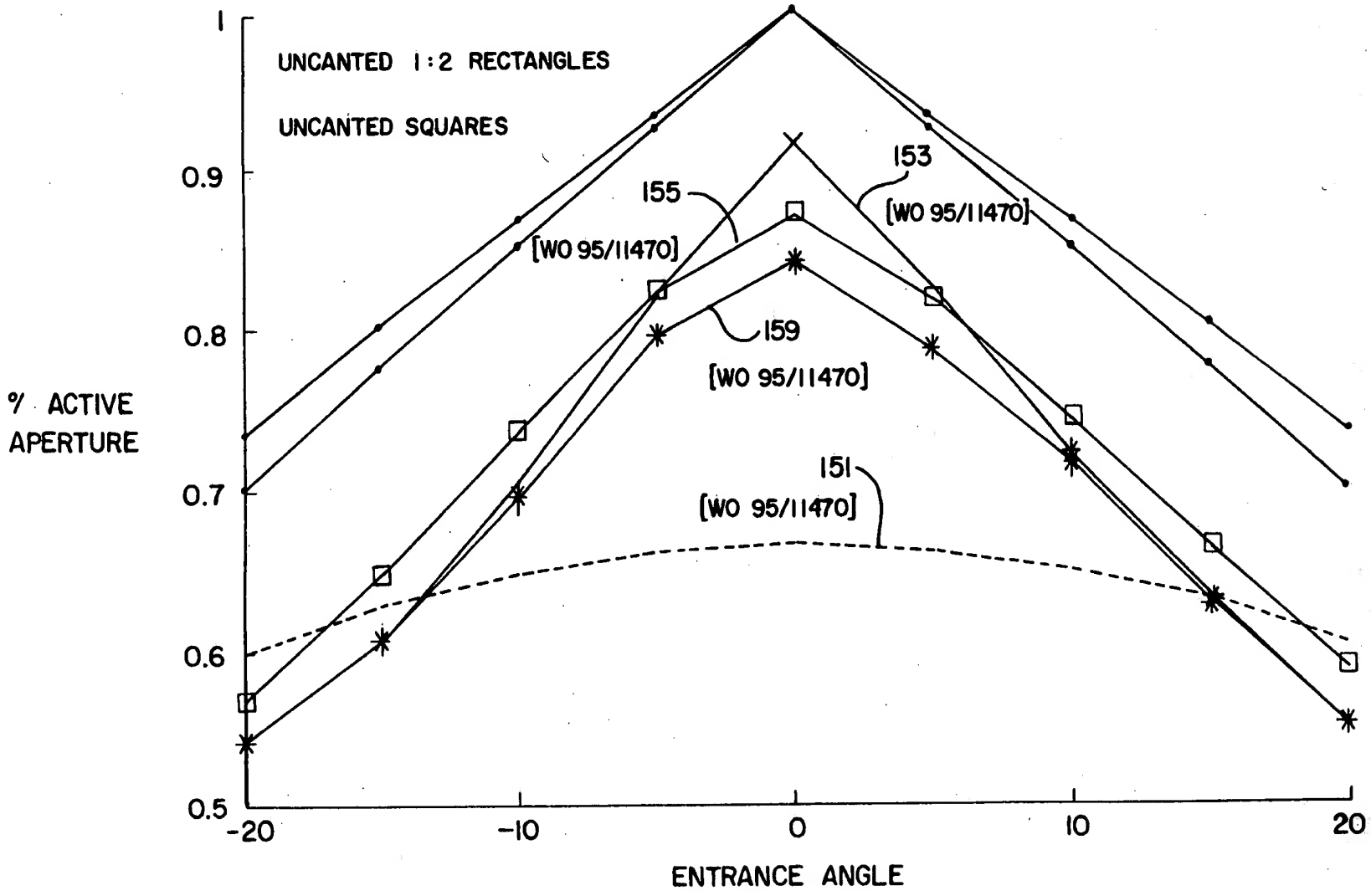

FIG. 45

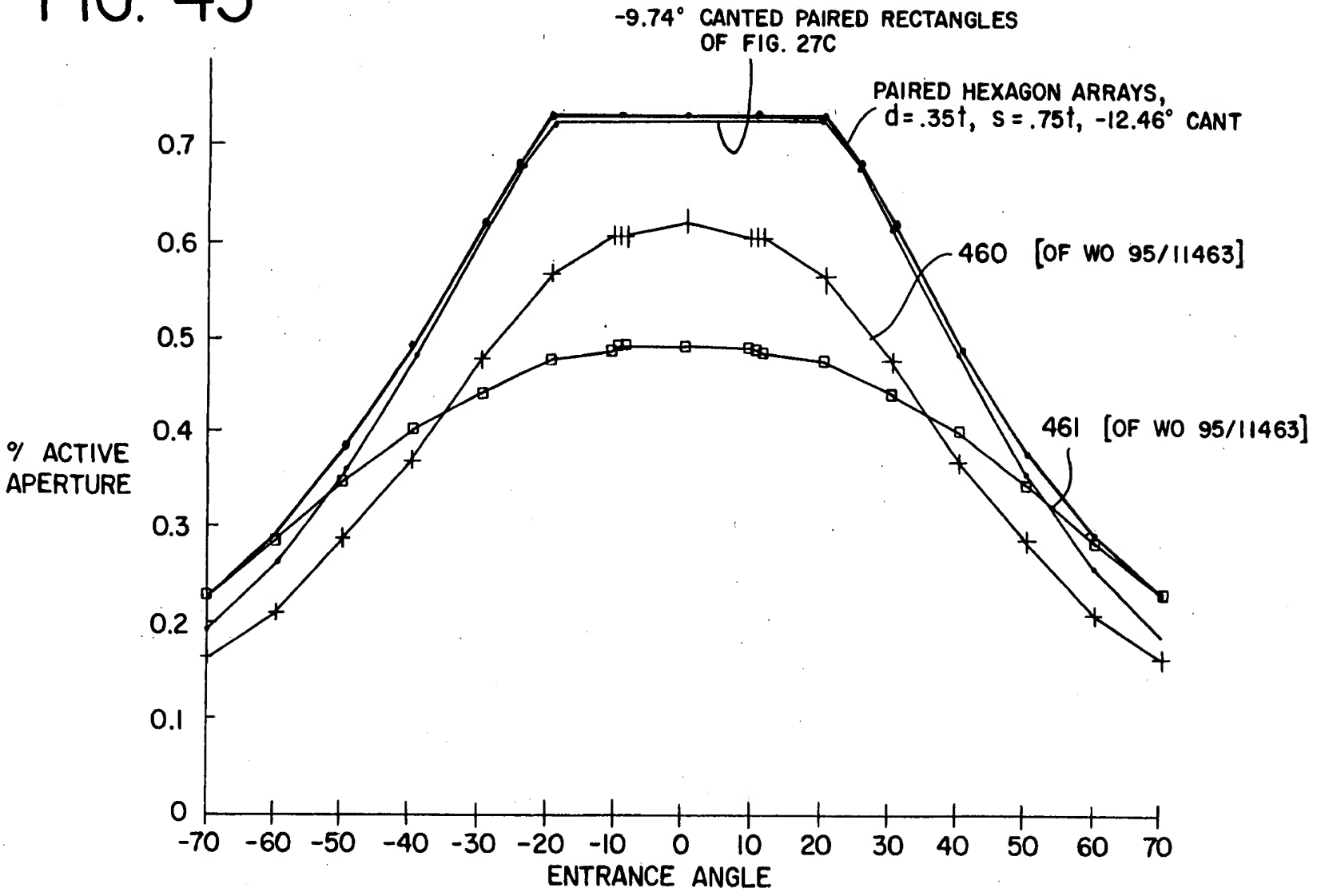
-9.74° CANTED PAIRED RECTANGLES
OF FIG. 27C
PAIRED HEXAGON ARRAYS,
d=.35t, s=.75t, -12.46° CANT
460 [OF WO 95/11463]
461 [OF WO 95/11463]
% ACTIVE APERTURE
0.7
0.6
0.5
0.4
0.3
0.2
0.1
0
-70 -60 -50 -40 -30 -20 -10 0 10 20 30 40 50 60 70
ENTRANCE ANGLE

FIG. 46a

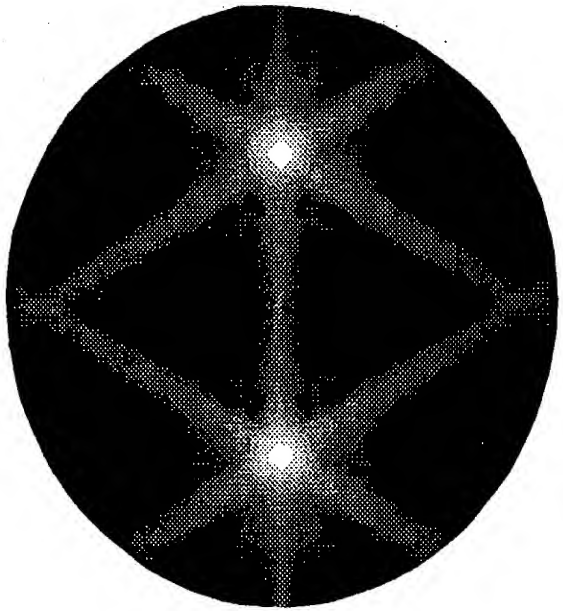

FIG. 46b

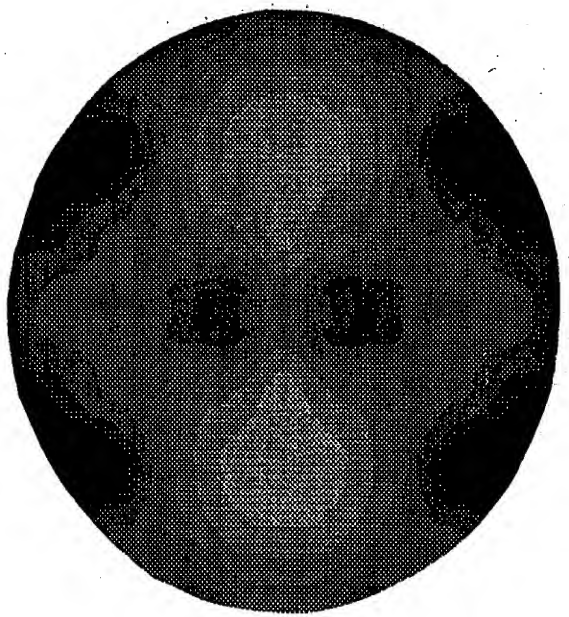

FIG. 46c